2004

NASA FACULTY FELLOWSHIP PROGRAM

MARSHALL SPACE FLIGHT CENTER

THE UNIVERSITY OF ALABAMA
THE UNIVERSITY OF ALABAMA IN HUNTSVILLE
ALABAMA A&M UNIVERSITY

LOCAL INTENSITY ENHANCEMENTS IN SPHERICAL MICROCAVITIES: IMPLICATIONS FOR PHOTONIC CHEMICAL AND BIOLOGICAL SENSORS

Prepared By:	Kirk A. Fuller
Academic Rank:	Research Scientist
Institution and Department:	University of Alabama in Huntsville Earth System Science Center
NASA/MSFC Directorate:	Biological and Physical Sciences
MSFC Colleague:	Dr. David D. Smith

Introduction

In this report, we summarize recent findings regarding the use spherical microcavities in the amplification of light that is inelastically scattered by either fluorescent or Raman-active molecules. This discussion will focus on Raman scattering, with the understanding that analogous processes apply to fluorescence.

Raman spectra can be generated through the use of a very strong light source that stimulates inelastic light scattering by molecules, with the scattering occurring at wavelengths shifted from that of the source and being most prominent at shifts associated with the molecules' natural vibrational frequencies. The Raman signal can be greatly enhanced by exposing a molecule to the intense electric fields that arise near surfaces (typically of gold or silver) exhibiting nanoscale roughness. This is known as surface-enhanced Raman scattering (SERS). SERS typically produces gain factors of $10^3 - 10^6$, but under special conditions, factors of $10^{10} - 10^{14}$ have been achieved (Felidj, 2003).

An intriguing mechanism for near-field enhancement arises from microcavity whispering gallery modes (WGMs). Also known as morphology-dependent resonances (MDRs), these modes appear at sharply defined spectral positions for any sufficiently large and lossless spherical particle. (MDRs also appear in cylindrical and spheroidal microstructures.) A key feature of a resonator is its quality factor Q, which is the ratio of stored energy to the energy lost per cycle through the cavity. Microspheres can sustain Qs approaching 10^{10} (cf. Vernooy et al., 1998). The dramatic increases in photon densities within these microcavities have been shown to produce low-threshold nonlinear optical effects such as stimulated Raman scattering, lasing, spectral hole burning, and cavity quantum electrodynamic effects. In addition to very high photon densities in the mode volumes of microcavities, very strong evanescent fields reside on and near their outer surfaces. Vigorous research has begun into ways to use these strong surface fields to detect and analyze minute amounts of molecular species adsorbed onto the resonator. Optical shifts in MDRs have been used to detect adsorption of proteins onto glass spheroids and resonant enhanced evanescent wave fluorescence has been proposed for photonic biosensing, as have integrated optical microcavities.

Calculations presented below indicate that the absorption cross sections of metal nanoparticles immobilized onto dielectric microspheres can be greatly enhanced by cavity resonances in the microspheres. Molecules attached to the immobilized nanoparticles would thus experience cascaded surface-photoenhancements (CSPs), leading to increased gains in Raman scattering of several orders of magnitude over conventional SERS effects. Gain factors of $10^3 - 10^4$ are predicted for realistic, though challenging, experimental conditions using homogenous microspheres. Our calculations further indicate that carefully structured cladded microspheres, acting as coupled microcavities, could produce a further gain of 3 or 4 orders of magnitude. Cascaded surface photoenhancement thus has the potential of pushing sensitivities of chemical and biological detectors to dramatically lower thresholds.

Enhanced absorption by nanoparticles on a microcavity

The electric field at any point may be expanded in vector spherical harmonics $\mathbf{N}_{np}$. The vector spherical harmonics may be written as $\mathbf{N}_{np} = Rg\mathbf{N}_{np} + i\,Ig\mathbf{N}_{np}$, where Rg and Ig stand for 'regular' (finite at the origin) and irregular. The expansion for the incident field (here, an infinite plane wave) is

$$\mathbf{E}^{\text{inc}} = \sum_{np} q_{np}\, Rg\mathbf{N}_{np}, \tag{1}$$

and for the external and internal fields of a homogeneous sphere, respectively,

$$\mathbf{E}^{\text{sca}} = \sum_{np} q_{np}\, a_{np}\, \mathbf{N}_{np}, \tag{2}$$

$$\mathbf{E}^{\text{cor}} = \sum_{np} q_{np}\, c_{np}\, Rg\mathbf{N}_{np} \tag{3}$$

where the expansion coefficients a_{np} and a_{np} are functions of the sphere's refractive index m, radius a, and the wavelength λ. These coefficients and the q_{np} are well-known (cf. Fuller and Mackowski, 2000), and are also used in calculating the cross sections for scattering and absorption, C_{sca} and C_{abs}, respectively.

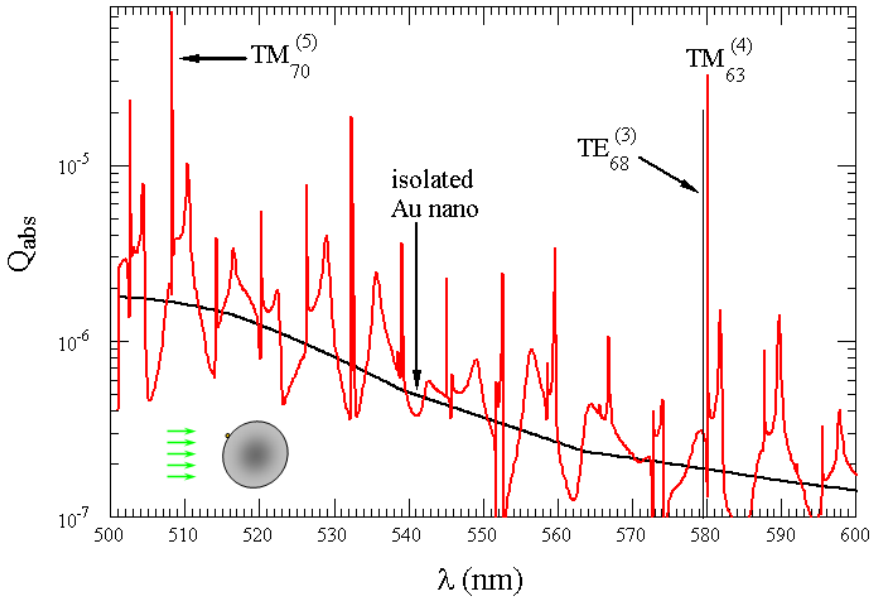

Figure 1: Absorption efficiency spectrum of a 10 nm Au sphere on a 5 μm latex microbead. The position of the nanoparticle (not drawn to scale) relative to the incident beam is shown in the inset in the lower left corner of the graph. The absorption efficiency of the nanoparticle in the absence of the sphere is given by the black curve. The calculations are based on an exact formulation for compounded sphere systems (Fuller and Mackowski, 2000).

Figure 1 shows how the absorption efficiency Q_{abs} (= C_{abs} divided by, in this case, the microsphere's geometric cross section) of a Au nanoparticle may be enhanced near the surface of a microcavity as the wavelength of the incident beam is tuned through a series of microsphere WGMs. There is no absorption in the microsphere itself, and so this graph shows that the Au nanoparticle is being exposed to greatly enhanced local intensities.

For illustrative purposes, latex beads were chosen as the microcavities for this calculation. In practice, one must choose microcavities that are made from materials, such as silica, that will not themselves produce a strong Raman background signal. The Q_{abs} spectra and local energy densities will be similar for equivalent modes, regardless of the dielectric chosen.

The electromagnetic 'terrain' responsible for this resonance-enhanced absorption is shown in Fig. 2, which is a plot of the ratio of the energy density near or in the microcavity to that of the incident field. This calculation was made with an existing version of the author's computer program for scattering and absorption by a sphere. That this is a 3rd-order resonance may be inferred from the presence of three concentric rings in the mode volume of the cavity.

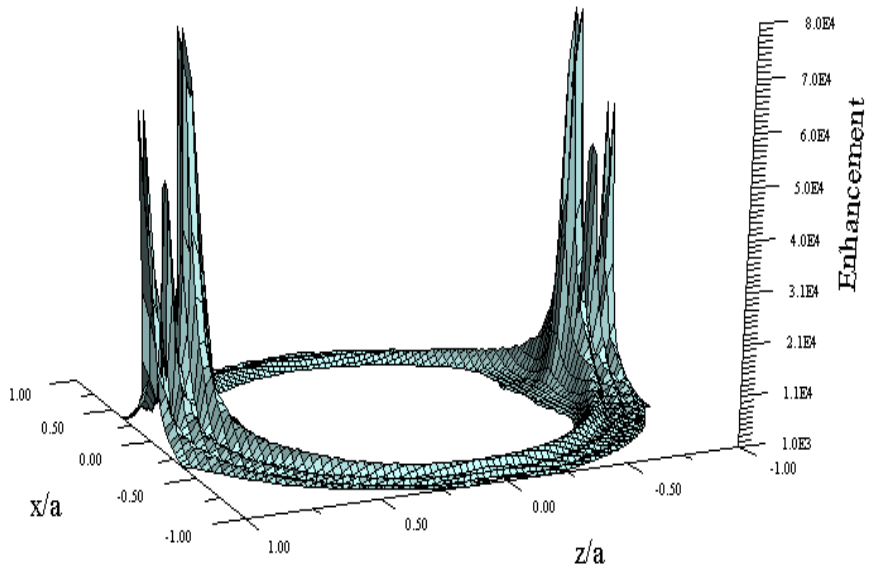

Figure 2: Electromagnetic energy density in the equatorial plain of a microsphere tuned to a 3rd-order TE_{69} resonance. The incident field propagates parallel to the z-axis. In order to better illustrate the structure of the mode volume of the resonance, only enhancements of greater than 10^3 are shown.

Internal and near fields of homogeneous and core-shell microspheres on resonance

The geometry of the problem is illustrated in Figure 3 for the case of a sphere with a concentric spherical inclusion. The field associated with a particular n may be written as a sum of partial waves multiply reflected between the surface of the core and the outer (concave) surface of the shell. Defining

$$f_{np} = \frac{c_{np}}{1 - {}^2a_{np}\,\breve{a}_{np}} \tag{4}$$

we have shown (Fuller and Smith, 2003) that the fields in the core and shell may be written, respectively, as

$$\mathbf{E}^{\mathrm{shl}} = \sum_{np} q_{np}\, f_{np}\, \left(Rg\mathbf{N}_{np} + {}^2a_{np}\,\mathbf{N}_{np}\right) \quad \text{and} \quad \mathbf{E}^{\mathrm{cor}} = \sum_{np} q_{np}\, f_{np}\, {}^2c_{np}\, Rg\mathbf{N}_{np}. \tag{5}$$

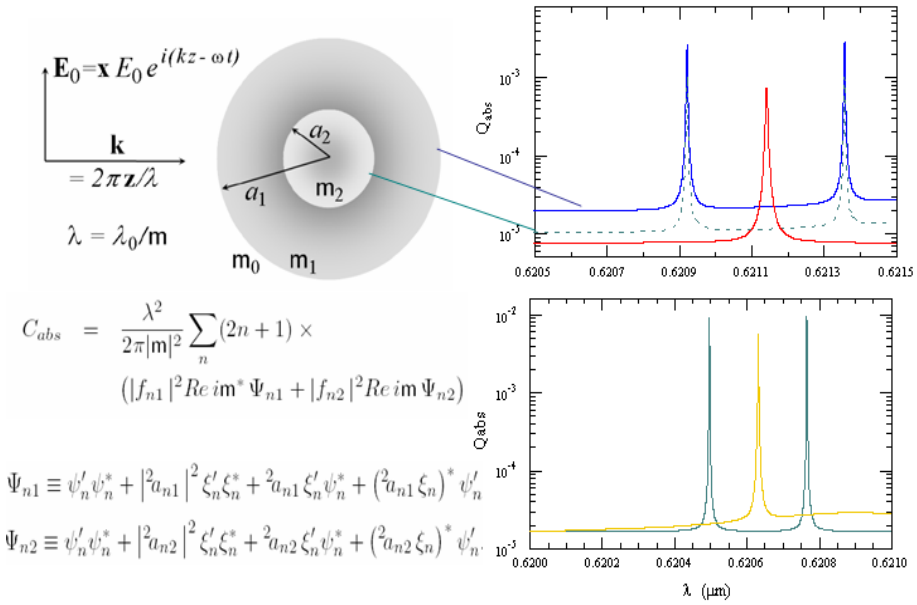

Figure 3: Geometry of the core-shell problem along with two illustrations of mode splitting by coupled concentric microcavities that have been tuned to co-resonance. The equation for the absorption cross section at a particular distance from the center of the microcavity is also provided, and was developed by Fuller and Smith (2003). Evaluation of the equation at the outer surface of the shell and at the surface of the core then gives the total absorption cross section of the layered sphere and of the core, respectively. The difference of these two cross sections then gives the absorption cross section of the shell.

Also shown in Fig. 3 is the spectrum of slightly absorbing microcavities. The mode splitting displayed Fig. 3 is potentially of great consequence to the future development of Raman-based detection and analysis: The enhancement of the intensity of Raman scattering by metal nanoparticles is expressed in terms of incident and scattered local electric field amplitudes E_{loc} as

$$I_{SERS} \propto G_{SERS} \propto \frac{|E_{loc}(\omega_{exc})|^2}{|E_0(\omega_{exc})|^2}\frac{|E_{loc}(\omega_{RS})|^2}{|E_0(\omega_{RS})|^2,} \tag{6}$$

where ω_{exc} and ω_{RS} are the circular frequencies of the incident (excitation) and Raman scattered light, respectively. Excitation of the nanoparticle-microsphere systems discussed above results in a gain of

$$|E_{loc}(\omega_{exc})|^2/|E_0(\omega_{exc})|^2 \approx 10^2 - 10^4. \tag{7}$$

If, however, one were able to tune coupled cavity resonators to co-resonance, such that the excitation frequency coincided with the left peak in Fig. 3 and the right peak were centered on a Raman-active band, then that spectral feature would be amplified by a factor of $10^4 - 10^8$ *beyond* the gain already realized from SERS alone.

Fig. 4 provides a view of the local intensity enhancement for both homogeneous and co-resonant concentric microcavities. For this part of the work, the author's computer program for calculating scattering and absorption by a homogeneous sphere was modified to allow calculation of the internal and near fields of core-shell systems. The modifications were made in a way that should allow for easy extension of the program to the case of multilayered structures.

Figs. 3 and 4 as well as Figs. 1 and 2 indicate that an order-of-magnitude jump in absorption efficiency relates roughly to an order-of-magnitude increase in $|\mathbf{E}|^2$ near the surface of the cavity and so the absorption spectrum of a nanoparticle on the surface of the microsphere may be used to predict SERS gain factors. Calculations also indicated that coupling between the nanoparticle and the resonator will spoil the cavity Q if the diameter of the Au particle exceeds ≈ 150 nm. Also from Figs. 2 and 4 it should be noted that considerably larger (by yet another order of magnitude) gain factors are present near the poles of the microcavities.

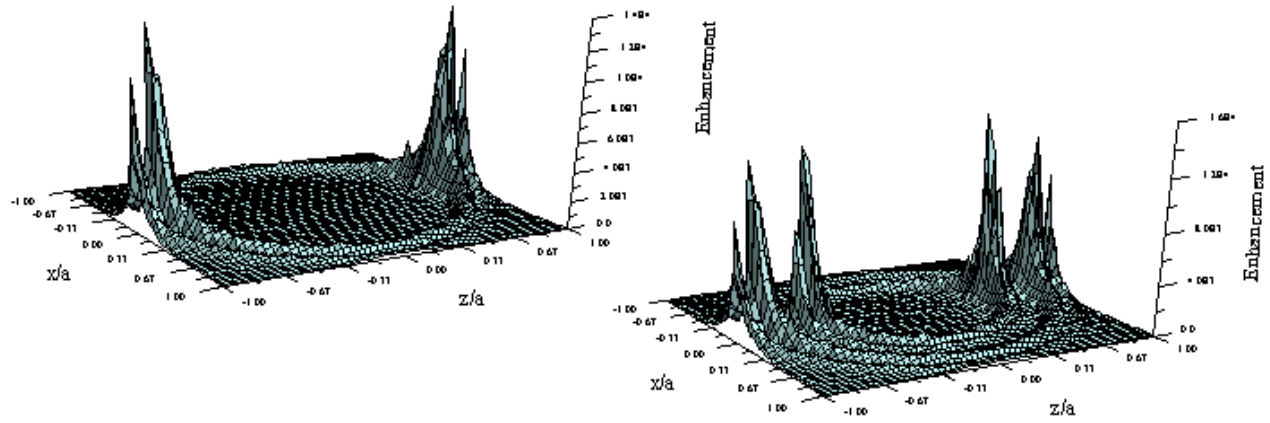

Figure 4: Enhancement factors in resonant homogeneous sphere and in co-resonant core-shell microcavity

Acknowledgments

The author wishes to express his great appreciation for the many valuable discussions with Dr. David D. Smith, and for the productive environment provided by MSFC for the performance of this research.

References

Félidj, N., J. Aubard, G. Lévi, J. R. Krenn, A. Hohenau, G. Schider, A. Leitner, and F. R. Aussenegg, Optimized surface-enhanced Raman on gold nanoparticle arrays, Appl. Phys. Lett. **82** 3095–3097(2003).

Fuller, K. A. and D. W. Mackowski, "Electromagnetic Scattering by Compounded Spherical Particles," in *Light Scattering by Nonspherical Particles*, M. I. Mishchenko, J. W. Hovenier, and L. D. Travis, Eds., Academic Press, NY 2000.

Fuller, K. A. and D. D. Smith, 'Partial wave analysis of coupled photonic structures,' in The 2002 NASA Faculty Fellowship Program Reasearch Reports, J. Bland Ed., Marshall Space Flight Center, 2003.

Smith, D. D. and K. A. Fuller, Photonic bandgaps in Mie scattering by concentrically stratified spheres, accepted for publication, J. Opt. Soc. Am. B, **19** No. 10. (2002).

Vernooy, D. W., V. S. Ilchenko, H. Mabuchi, E. W. Streed, and H. J. Kimble, High-Q measurements of fused-silica microspheres in the infrared, Opt. Lett. **23**, 247–249(1998)